

Low-temperature spin dynamics of a valence bond glass in Ba_2YMoO_6 .

M A de Vries¹, J O Piatek², M Misek³, J S Lord³,
H M Rønnow², J-W G Bos⁵

E-mail: m.a.devries@ed.ac.uk

¹ School of Chemistry, The University of Edinburgh, Edinburgh EH9 3JJ, UK.

² Laboratory for Quantum Magnetism, École Polytechnique Fédérale de Lausanne (EPFL), Switzerland.

³ School of Physics, The University of Edinburgh, Edinburgh, EH9 3JZ, UK.

⁴ ISIS Facility, Rutherford Appleton Laboratory, Chilton, Didcot, Oxon OX11 0QX, UK.

⁵ Department of Chemistry - EPS, Heriot-Watt University, Edinburgh, EH14 4AS, UK.

Abstract. We carried out AC magnetic susceptibility measurements and muon spin relaxation spectroscopy on the cubic double perovskite Ba_2YMoO_6 , down to 50 mK. Below ~ 1 K the muon relaxation is typical of a magnetic insulator with a spin-liquid type ground state, i.e. without broken symmetries or frozen moments. However, the AC susceptibility revealed a dilute-spin-glass like transition below ~ 1 K. Antiferromagnetically coupled $\text{Mo}^{5+} 4d^1$ electrons in triply degenerate t_{2g} orbitals are in this material arranged in a geometrically frustrated fcc lattice. Bulk magnetic susceptibility data has previously been interpreted in terms of a freezing to a heterogeneous state with non-magnetic sites where $4d^1$ electrons have paired in spin-singlets dimers, and residual unpaired $\text{Mo}^{5+} 4d^1$ electrons. Based on the magnetic heat capacity data it has been suggested that this heterogeneity is the result of kinetic constraints intrinsic to the physics of the pure system (possibly due to topological overprotection), leading to a self-induced glass of valence bonds between neighbouring $4d^1$ electrons. The μSR relaxation unambiguously points to a static heterogeneous state with a static arrangement of unpaired electrons isolated by spin-singlet (valence bond) dimers between the majority of $\text{Mo}^{5+} 4d$ electrons. The AC susceptibility data indicate that the residual magnetic moments freeze into a dilute-spin-glass-like state. This is in apparent contradiction with the muon-spin decoupling at 50 mK in fields up to 200 mT, which indicates that, remarkably, the time scale of the field fluctuations from the residual moments is ~ 5 ns. Comparable behaviour has been observed in other geometrically frustrated magnets with spin-liquid-like behaviour and the implications of our observations on Ba_2YMoO_6 are discussed in this context.

PACS numbers:

1. Introduction

Geometrical frustration of the exchange interactions in antiferromagnetic (Mott) insulators with magnetic topologies based on triangles and tetrahedra can fully suppress the spontaneous symmetry breaking to the common long-range ordered antiferromagnetic (Néel) state [1, 2]. Quantum-ordered spin-liquid states are widely expected to occur in such system. These could be gapless, with emergent Fermionic quasiparticles called spinons with $S = 1/2$ and no charge or gapped (topologically-ordered) [3, 4]. A number of materials with a spin-liquid-like absence of frozen moments have now been identified [5, 6, 7, 8, 9]. These are without exception gapless, often still display some weak hysteretic behaviour below 2 K, and have only short-ranged dynamic magnetic correlations [10, 11, 8] which is contrary to theoretical expectations of gapless spin liquids.

While these short-ranged correlations could in some cases be due to disorder [10, 8], another plausible explanation is the presence of kinetic constraints towards freezing into the (quantum) ground state [12, 13, 14, 15]. It has been shown that even where quantum fluctuations are so strong that no local order parameters exist, as in some geometrically frustrated quantum magnets, these quantum fluctuations are not always effective for equilibration to its true quantum ground state [12, 13, 14, 15]. When the width of the tunnelling barriers becomes comparable to the system size, out-of-equilibrium quantum-glassy phases can stabilize [12, 13, 14]. Quantum spin systems with strictly local interactions, with local degrees of freedom coupled to a heat bath (Mott insulators), also studied in the context of fault-tolerant quantum computation [16], are ideal model systems to study this quantum glassiness [12]. A particularly intriguing and far-reaching possibility are that there are kinetic constraints due to “topological overprotection” [12, 14]. The topological order [17] in a gapped quantum (spin liquid) state is known to lend the ground state a certain rigidity and “protect” the quantum wavefunction against decoherence and material imperfections [18, 16]. An infinite number of local operations would be required to mess up the macroscopic entanglement of this quantum ordering. In Mott insulators this concept can be turned on its head; here the physics is local [19] and hence the only route to access any topologically-ordered states in the first place, is via an infinite number of local operations. This has been termed “topological overprotection” [12, 14]. Within this context we studied the cubic fcc lattice antiferromagnet Ba_2YMoO_6 , which has previously been suggested [20] to freeze into a valence bond glass (VBG) state [21]. This is in line with theoretical predictions for a quantum magnet with an fcc lattice predicting a “strong glass” state due to topological overprotection [12, 14]. However, the Hamiltonian of this cubic perovskite with unquenched orbital degrees of freedom is significantly more complex than that of the Heisenberg Hamiltonian, as was recently pointed out [22].

Ba_2YMoO_6 is a double perovskite (of general formula $\text{A}_2\text{BB}'\text{O}_6$) where the two B-site cations have assumed rocksalt order [23] (Fig. 1a). Magic-angle spinning NMR was reported to point to 3 % cation disorder [24] but in neutron diffraction data of our

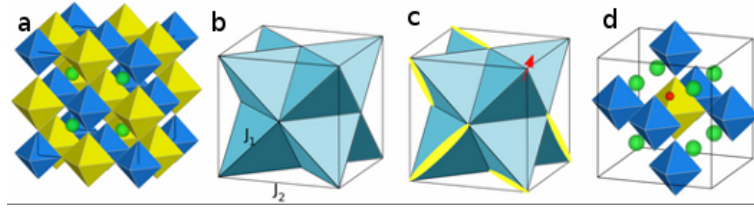


Figure 1. (Color online) (a) The Ba_2YMoO_6 double perovskite structure, showing the rocksalt ordering of MoO_6 octahedra (blue) and YO_6 octahedra (yellow) with Ba^{2+} (green) at the perovskite A site. (b) The network of edge-sharing tetrahedra of the fcc antiferromagnet. (c) An illustration of the valence bond glass state, with the non-magnetic spin singlet dimers across random edges (yellow) and a single unpaired spin (red). (d) The muon stopping site (red) on an edge of the YO_6 octahedron, surrounded by 6 MoO_6 octahedra.

sample the B-site ordering of the Mo/Y cations refines to 100(1)% 15, as expected for the large difference in ionic radii of the Y^{3+} and Mo^{5+} of 0.29 Å. The Mo^{5+} cations have a single unpaired electron in an octahedral crystal field and are separated from each other by 90° Mo-O-O-Mo bonds (J_1) along the edges of corner-sharing tetrahedra, and 180° Mo-O-Y-O-Mo bonds (J_2) (Fig. 1b). The 12 near-neighbour (J_1) bonds and 6 further neighbour bonds per site lead to a strong net antiferromagnetic interaction, with a Weiss temperature of -143(5) K. Ba_2YMoO_6 remains cubic (space group $\text{FM}\bar{3}\text{m}$) down to at least 2 K which means the single $4d$ t_{2g} electron is also orbitally degenerate. Due to relatively strong spin-orbit coupling in the $4d$ shell this degeneracy is expected to be partially lifted, leading to $J = 3/2$ quadruplets [22]. It is noteworthy that of the related compounds where the Y^{3+} is replaced for a trivalent lanthanide ion only in the case of Nd^{3+} and Sm^{3+} a Jahn-Teller distortion is observed to a tetragonal unit cell, and in both cases this distortion is accompanied by antiferromagnetic ordering [23]. The actual Hamiltonian that applies to Ba_2YMoO_6 is not reproduced here for brevity. It contains antiferromagnetic and ferromagnetic exchange interactions that depend on the orientations of the occupied orbital states within the degenerate t_{2g} manifold, a quadrupolar interaction between neighbouring orbitals and a spin-orbit coupling term which can be projected-out by constraining the system to a low-energy subspace with $J = 3/2$ moments [22]. A (naïve) estimate of the orbital-dependent 15 nearest-neighbour antiferromagnetic exchange interaction strength J_1 , assuming further-neighbour interactions can be neglected, yields $|J_1| \sim 72$ K.

Remarkably, the magnetic/electronic heat capacity of the single $4d$ t_{2g} electron at the Mo site evidenced a pseudogap below ~ 50 K, gradually locking up most of the magnetic entropy of the $J = 3/2$ moments [20]. This “strong glass”-like freezing does however not translate to a significantly increased muon relaxation down to 2 K, indicating that most of the Mo^{5+} $4d$ electrons pair up with near-neighbour spins to form non-magnetic spin-singlet- or valence bond dimers [20] (Fig. 1c). A second Curie-Weiss regime is observed in the DC susceptibility below 25 K, with a Weiss

temperature of $-2.6(2)$ K. The paramagnetic susceptibility between 1.9 and 7 K was found to be equivalent to that from $8(1)\%$ of the Mo^{5+} magnetic moments as measured at high temperature (see supplementary information). These residual, apparently weakly-coupled spins (sometimes referred to as “orphan spins”) are often observed in geometrically-frustrated compounds [25]. In some cases this has been suggested to be spins left-out from spin-singlet valence-bond dimerizations between the majority of spins, leaving a small fraction of magnetically-isolated and thus weakly-interacting unpaired-spin moment [26, 10] (Fig. 1c). Hence, “dangling spins” might in this case be a better term. The aim of the present study was to characterise the low-temperature spin-orbital dynamics to confirm the VBG proposal.

2. Results

The polycrystalline sample was synthesised using a solid state synthesis method as described in [20]. AC magnetic susceptibility measurements were carried out using an inductive susceptometer from CMR-direct in an Oxford Instruments dilution fridge (down to 50 mK) and in a 3He fridge (down to 300 mK). The measurements used an AC field of 0.02 mT in a frequency range from 54.5 to 8900 Hz. The intensity of the AC susceptibility signal at all frequencies was assumed to match the low-temperature DC susceptibility obtained using a SQUID magnetometer [see supplementary information]. As shown in Fig. 2a,b frequency-dependent cusps are observed around 600 mK in both the dispersive (χ') and dissipative (χ'') parts of the dynamic susceptibility. The frequency dependence of T_{max} (Fig. 2c) exhibits Arrhenius-activated behaviour (the straight line in Fig. 2c), with an activation energy $E_a = 39(2)$ K and a trial frequency $f_0 \sim 1 \times 10^{29}$ Hz. Such a frequency dependence in the AC susceptibility is a defining feature of a strong glass as well as spin glasses [27]. Figure 2d shows the effect of an additional DC field on the AC susceptibility at the spin-glass transition, revealing only a modest suppression of the AC susceptibility in fields below 250 mT. The AC magnetic susceptibility is a macroscopic property. We complemented this data with muon spin relaxation spectroscopy which is a local probe of the spin dynamics in the material, using the MUSR instrument at the ISIS facility, UK. Figure 3a shows the average time dependence of the spin polarisation of muons implanted in a 3 g powder sample, for a selection of temperatures between 50 mK and 120 K and in zero external field. Figure 3b shows the field dependence of the muon relaxation at 50 mK, for (longitudinal) magnetic fields applied along the initial muon spin polarisation direction.

At the time the muons are implanted in the sample ($t = 0$), all muon spins point along the forward (z) direction. The muon spins will then precess due to the local fields at the muon sites. In a material with uniform magnetic order all muons will precess with the same frequency, which translates to an oscillation of the muon polarisation $P_z(t)$. In the case of static disordered moments a single damped oscillation is observed equilibrating to 1/3rd of the initial polarisation, corresponding to on average 1/3rd of the randomly orientated magnetic moments that are aligned with the initial muon

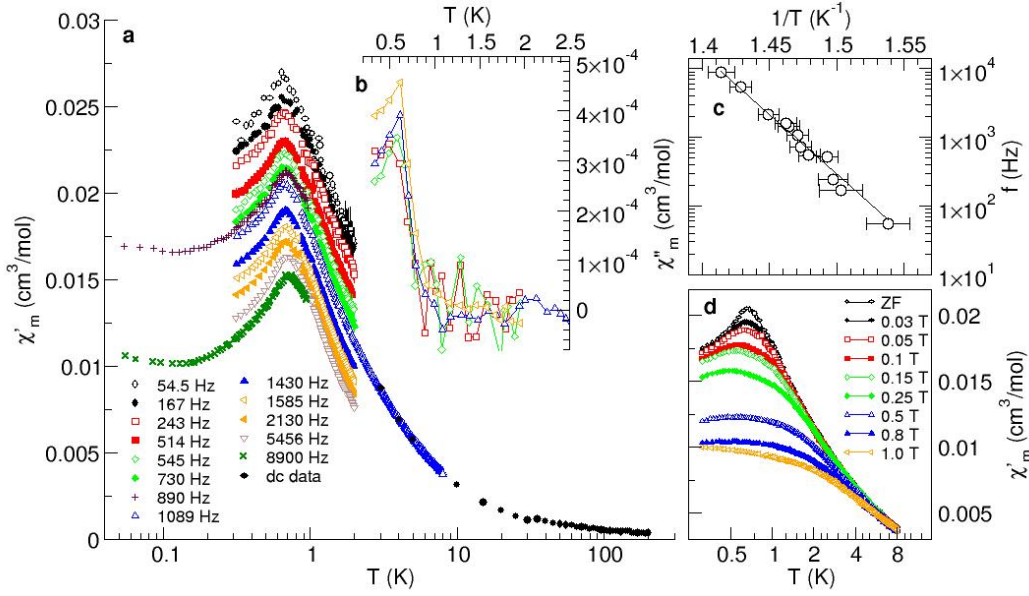


Figure 2. (Color online) AC magnetic susceptibility measured in a dilution refrigerator. (a) The frequency dependence of dispersive (real) part of the AC susceptibility at low temperatures matched to the DC susceptibility. (b) The dissipative (imaginary) part of the AC susceptibility near the spin-glass transition. (c) The Arrhenius-activated frequency dependence of the temperature with maximum AC susceptibility (T_{max}) (see text) (d) The effect of DC fields up to 1 T on the AC susceptibility (at 1029 Hz) near the transition temperature.

spin polarisation and hence do not cause muon precession or depolarisation. This type of relaxation is observed, for example, below the spin-glass transition in the related compound $\text{Sr}_2\text{MgReO}_6$ with Re^{6+} $S = 1/2$ [28]. The muon relaxation in the presence of static but random fields can be suppressed by the application of a longitudinal magnetic field stronger than the local fields at the muon site. This enabled the determination of the contribution to the muon relaxation from nuclear spins $P_{\text{nuc}}(t)$ at the Y and at a fraction of the Ba and Mo sites in Ba_2YMoO_6 , which below ~ 10 K are static at the time scale of the muon experiment. At 1.3 K, just above the spin-glass transition observed in the AC susceptibility data, a 5 mT field was sufficient to decouple the muon relaxation for the small nuclear fields (typically up to 1 mT), yielding the nuclear relaxation factor $P_{\text{nuc}}(t)$ as shown in Fig. 3b. The observed nuclear relaxation is as expected for the muon stopping site on the edges of the YO_6 octahedra [29] (Fig. 3d, see supplementary information for further details). No further change in the muon relaxation was observed with the application of longitudinal fields up to 200 mT, confirming that the remaining muon relaxation was due to larger (non-frozen) electronic moments. Well into the paramagnetic state the electron-spin fluctuations are usually too fast to be picked-up by muons leading to negligible muon relaxation at 120 K (Fig. 3a). As indicated by the heat capacity data, the entropy from most of the $J = 3/2$ moments is locked up below ~ 40 K. The very slow relaxation at 2 K thus confirms that the majority

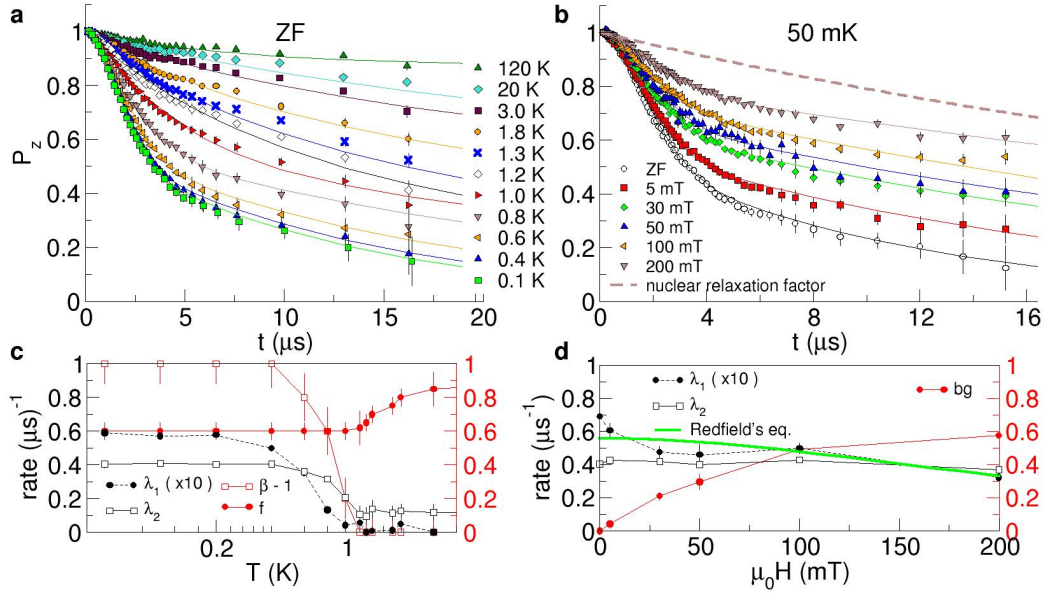


Figure 3. (Color online) Muon spin relaxation data obtained at MUSR, ISIS. (a) The temperature dependence of the zero- field muon relaxation ($P_z(t)$) between 50 mK and 120 K. (b) The field dependence of the muon relaxation at base temperature (50 mK) and the nuclear relaxation factor which was confirmed to be constant below 1.3 (See text and supplementary material). (c) The fit parameters for fits of Eq. 1 to the zero-field data as a function of temperature, taking into account the weak nuclear relaxation. (d) The fit parameters for fits of Eq. 1 to the 50 mK muon relaxation in fields up to 200 mT. The fluctuation rate was determined from the field dependence of λ_1 using Redfields equation (solid green line) (see text and supplementary information).

of these magnetic moments must have paired into non-magnetic spin-singlet or valence bond dimers [20]. Across the spin-glass transition the muon relaxation rate increases sharply but even at 400 mK, below which no further increase in the muon relaxation (depolarization) is observed, the relaxation rate remains remarkably low, even for a system with dilute electronic spins. Amongst antiferromagnetic insulators without a spin-gap, only in the spin-liquid compound herbertsmithite is a slower muon relaxation observed at 50 mK [6]. If this weak relaxation were due to static random moments, then the fields from these moments at the muon site would have to be as small as ~ 0.6 mT, so that the muon relaxation should be fully decoupled in a 5 mT field. As is clear from Fig. 3b, a 5 mT field only leads to a small reduction of the relaxation, the difference with the zero-field relaxation being given approximately by $P_{nuc}(t)$. A clear muon relaxation signal persists in fields up to 200 mT, consistent with the presence of fluctuating electronic magnetic moments.

The muon relaxation $P_z(t)$ is determined by the magnitude, variation and fluctuation of local fields inside a sample, and carefully analysing the shape of the muon relaxation curve can allow to distinguish different scenarios. Here we found that the best fitting scenario is with two different muon environments, designated E1 and

E2, with an exponential relaxation in E1 (arising from spin fluctuations with a rate λ_1 that will be estimated later), and a phenomenological modified-exponential decay with $1 \leq \beta \leq 2$ (for E2);

$$P_z(t) = P_{\text{nuc}}(t) \left[f e^{-\lambda_1 t} + (1 - f) \left(e^{-(\lambda_2 t)^\beta} + b \right) \right], \quad (1)$$

where $P_{\text{nuc}}(t) = 1$ for longitudinal fields ≥ 5 mT, f is the fraction of muons in E1 and the constant background $b = 0$ in zero-field. The results of the fits to the data down to 50 mK and in fields up to 200 mT are shown in Fig. 3c and d, respectively. The background contribution b in E2 is constrained by the condition that with the fields up to 200 mT applied here the fraction of muons in E1 and E2 should be constant, as implied by the AC susceptibility data in Fig. 2d. Just above the spin glass transition, at 1.3 K, the stretching exponent $\beta = 1$ and $\lambda_1 = 0$. This implies that a major fraction f of the muons is located in a non-magnetic environment (E1), while the remaining muons ($\sim 30\%$ at 1.3 K) undergo an exponential relaxation due to surrounding fluctuating spins (E2). On cooling through the spin-glass transition the depolarisation of the muons in E2 changes sharply from exponential to Gaussian, as previously observed in the $S = 3/2$ kagome antiferromagnet $\text{SrCr}_8\text{Ga}_4\text{O}_{19}$ [26], and the fraction of muons in E2 increases to 40(5)%. At the lowest temperatures accessed the muons in E1 also exhibit a weak exponential relaxation (Fig. 3c). At base temperature E1 and E2 correspond to muons surrounded by respectively 0 and 1 unpaired electron on the 6 Mo^{5+} ions surrounding the muon site. Non-magnetic (E1) and magnetic (E2) environments were also evident from ^{89}Y NMR [24] with a ratio of approximately 50:50, comparable to our results (Fig. 3c). This confirms that 1) the muon stopping site is near the Y^{3+} and 2) that the muon does not perturb the low-temperature dilute spin-glass state significantly. Because each muon on the Y site is surrounded by 6 Mo^{5+} ions, the fraction of muons in a non-magnetic environment of 0.60(5) implies that at low temperature (< 10 K) a fraction of 0.91(1) of the Mo^{5+} sites [$(0.91)^6 = 0.6$] are non-magnetic. Hence, only $\sim 9(1)\%$ of the Mo^{5+} carry a net magnetic moment at low temperature. Below 400 mK no further increase of the muon relaxation rates is observed down to 50 mK, indicating that thermal fluctuations do not play a major role at these temperatures. The spin fluctuation rate τ and magnitude Δ can in ideal cases be determined from the field dependence of the exponential muon relaxation rate λ_1 using Redfields formula [30] (see supplementary information). The field dependence of the exponential relaxation rate λ_1 in E1 at 50 mK as obtained from the data in Fig. 3b was fitted with Redfields formula (the green line in Fig. 3d, see also supplementary material), yielding a fluctuation time scale of 5(2) ns, with a field distribution Δ of 2.2(1) mT. This field-strength is as expected for muons in E1, without directly neighbouring unpaired spins. These muons probe the average fluctuating magnetic field from many distant unpaired electrons.

3. Discussion

Our analysis of the muon data rules out any major rearrangement of the unpaired spins over the available Mo sites within the time scale of the muon experiment of 16 μ s. Dynamical models of fluctuating valence bonds, where the orphan- or dangling spins are mobile, as proposed for $SrCr_8Ga_4O_{19}$ [26] have been explored but can in the case of Ba_2YMoO_6 be ruled out because of the much larger fraction of dangling spins, while at the same time the muon relaxation is more than an order of magnitude slower than for $SrCr_8Ga_4O_{19}$ [26]. Such models predict a fast $t = 0$ muon relaxation for a significant fraction of the muons, which is not observed; the $t = 0$ asymmetry at 50 mK and 120 K are comparable. Hence, the low temperature state in Ba_2YMoO_6 is static inhomogeneous state without any sign of local order parameters down to 50 mK. This state contains non-magnetic sites where the neighbouring $Mo^{5+} 4d^1$ electrons must have paired up in non-magnetic spin-singlets, and residual unpaired spins. A VBG state, as previously proposed [20], provides a natural explanation for this inhomogeneous state. However, a larger than previously estimated [24, 20] amount of Mo/Y antisite disorder would also explain the presence of residual unpaired spins at fixed locations. Hence, of all data so far available on Ba_2YMoO_6 the strongest evidence in favour of a VBG is the heat capacity [20]. As pointed out earlier, the pseudogap in the heat capacity [20] below 50 K (also visible in the neutron spectra [11]) points to a gradual, strong-glass, freezing at temperatures comparable to the magnetic exchange interaction $|J_1|$ of ~ 73 K. Hence, it must be the readiness of each $4d$ electron to randomly form a near-neighbour valence bond with one of its 12 near neighbours at high temperature, that prevents freezing into a (quantum-) ordered structure at low temperature. This type of behaviour is also characteristic of structural glass formers. It is also thought that disorder, even a very small amount, can stabilise a VBG state [21, 31], although in other cases disorder is known to reduce kinetic constraints towards nucleation of the thermodynamic state. An intriguing question that therefore remains is whether the thermodynamic state would be a topologically ordered state, in which case the kinetic constraints stabilising the VBG are due to topological overprotection, or an orbitally ordered state leading to a structural distortion from cubic to tetragonal symmetry at low temperature. It should in this respect be noted that the latter is observed in the closely related materials Ba_2NdMoO_6 and Ba_2EuMoO_6 , while analogues with Gd, Dy, Er, Yb have a magnetic susceptibility similar to that of Ba_2YMoO_6 [23].

We now turn to the observations on the $\sim 8\%$ of residual unpaired spins, that account for the low-temperature magnetic susceptibility. The Arrhenius-activated behaviour in the low-temperature AC susceptibility indicates that these spins freeze into a dilute-spin-glass-like state, with thermally-activated collective dynamics at the macroscopic scale. This implies that these spins interact via a weak residual exchange coupling (dipolar couplings would lead to freezing at still lower temperatures), and are randomly distributed over the Mo sites. It is surprising that even for muons directly neighbouring these unpaired spins the relaxation down to 50 mK remains extremely

slow; if the residual spins giving rise to the spin-glass response in the AC susceptibility were static at the time scale of the muon experiment, this would lead to fast relaxation of 2/3rd of the implanted muons well within $1\ \mu s$, as observed in dilute spin-glasses [32]. Less extreme examples where these apparently disparate behaviours coexist are known amongst geometrically frustrated magnets with ground states sometimes described as “quantum disordered” [25, 26]. The slow relaxation of the muons can only in part be explained by the large distance between the muon site and the nearest spin moments. A full understanding of this common behaviour in low-spin frustrated magnets is still outstanding. It is possible that the implanted muons perturb the fragile low-temperature spin-glass state, but this raises the question why below $\sim 10\ K$ the nuclear spins usually remain static on implantation of a muon. Zero-temperature fluctuations might also arise due to decoherence that affects ungapped quantum states. As a result the quantum glass state is best represented by a density matrix and not as a single wave function [12]. This is however unlikely to account for the difference in behaviour at microscopic and macroscopic scales. A third explanation that should be considered is that the explanation lies exactly in the difference of length scales; that the spin-glass freezing observed in the (macroscopic) magnetic susceptibility is truly an emergent property, while at microscopic length scales the spin dynamics is dominated by quantum fluctuations. These quantum fluctuations are in this case ineffective in equilibrating the system to its thermodynamic (quantum-) ordered ground state [12, 14, 13]. A time resolved coherent x-ray diffraction experiment on out-of-equilibrium states with local order parameters does suggest [33] that quantum fluctuations can at microscopic length scales occur at ns time scales, as also suggested by our data.

4. Conclusion

Our results confirm that the magnetic low-temperature state in Ba_2YMoO_6 without broken symmetries in the magnetic degrees of freedom is an inhomogeneous state. It could be dynamic but at a time scale that is slow compared to the time scale of the muon experiment of $10\ \mu s$, with the majority of spins paired into valence bonds. That this is a valence bond glass rather than a quantum spin liquid is in this case concluded from the electronic heat capacity [20]. The μSR experiment carried out here does not distinguish between a spin liquid and a valence bond glass; the relaxation is very similar to that reported for many materials presumed to have spin-liquid-like ground states [6]. This highlights the importance of the electronic/magnetic heat capacity to characterise materials with spin-liquid like ground states, providing for the present compound still the strongest confirmation of a VBG, while for the $2D\ S = 1$ antiferromagnet $Ba_3NiSb_2O_9$ the magnetic heat capacity clearly points to a spin liquid state [9]. In the absence of such data for the well-known kagome antiferromagnet spin liquid material herbertsmithite, it remains to be seen whether it is a spin liquid or a valence bond glass. The possibility of a VBG due to a small amount of disorder was put forward [31] following neutron spectroscopy data displaying below $120\ K$ temperature

independent short-ranged antiferromagnetic dynamic correlations [10], very much like the neutron spectrum observed for Ba_2YMoO_6 [11].

Acknowledgments

We would like to thank the Science and Technology Facilities Council for the provision of muon beamtime and Dr. P. King (ISIS) for assistance with the muon spectroscopy measurements at MUSR. We gratefully acknowledge discussions with Dr. P. J. Camp (Edinburgh), Dr. A. C. McLaughlin (Aberdeen) and Dr. C. Castelnovo (Cambridge) and helpful comments by Dr. J. Zaanen (Leiden). Part of this work was supported by funding from the Swiss National Science Foundation, MaNEP and Sinergia network MPBH.

References

- [1] Anderson P W 1987 *Science* **235** 1196–1198
- [2] Neel L 1936 *Ann. Phys.* **5** 232
- [3] Balents L 2010 *Nature* **464** 199–208 ISSN 0028-0836 URL <http://dx.doi.org/10.1038/nature08917>
- [4] Yan S, Huse D A and White S R 2011 *Science* **332** 1173–1176 URL <http://www.sciencemag.org/content/332/6034/1173.abstract>
- [5] Shimizu Y, Miyagawa K, Kanoda K, Maesato M and Saito G 2003 *Phys. Rev. Lett.* **91** 107001
- [6] Mendels P, Bert F, de Vries M A, Olariu A, Harrison A, Duc F, Trombe J C, Lord J S, Amato A and Baines C 2007 *Phys. Rev. Lett.* **98** 077204 (pages 4) URL <http://link.aps.org/abstract/PRL/v98/e077204>
- [7] de Vries M A, Stewart J R, Deen P P, Piatek J O, Nilsen G J, Rønnow H M and Harrison A 2009 *Phys. Rev. Lett.* **103** 237201
- [8] Nakatsuji S, Kuga K, Kimura K, Satake R, Katayama N, Nishibori E, Sawa H, Ishii R, Hagiwara M, Bridges F, Ito T U, Higemoto W, Karaki Y, Halim M, Nugroho A A, Rodriguez-Rivera J A, Green M A and Broholm C 2012 *Science* **336** 559–563 ISSN 0036-8075, 1095-9203 URL <http://www.sciencemag.org/content/336/6081/559>
- [9] Cheng J G, Li G, Balicas L, Zhou J S, Goodenough J B, Xu C and Zhou H D 2011 *Phys. Rev. Lett.* **107**(19) 197204 URL <http://link.aps.org/doi/10.1103/PhysRevLett.107.197204>
- [10] de Vries M A, Stewart J R, Deen P P, Ronnow H M and Harrison A 2009 Scale-free antiferromagnetic fluctuations in the $s=1/2$ kagome antiferromagnet herbertsmithite URL arXiv.org:0902.3194
- [11] Carlo J P, Clancy J P, Aharen T, Yamani Z, Ruff J P C, Wagman J J, Van Gastel G J, Noad H M L, Granroth G E, Greedan J E, Dabkowska H A and Gaulin B D 2011 *Physical Review B* **84** 100404 URL <http://link.aps.org/doi/10.1103/PhysRevB.84.100404>
- [12] Chamon C 2005 *Physical Review Letters* **94** 040402 URL <http://link.aps.org/doi/10.1103/PhysRevLett.94.040402>
- [13] Markland T E, Morrone J A, Berne B J, Miyazaki K, Rabani E and Reichman D R 2011 *Nature Physics* **7** 134–137 ISSN 1745-2473 URL <http://www.nature.com.ezproxy.webfeat.lib.ed.ac.uk/nphys/journal/v7/n2/full/nphys1865.html>
- [14] Castelnovo C and Chamon C 2011 *Phil. Mag.* **92** 304–323 ISSN 1478-6435 URL <http://www.tandfonline.com.ezproxy.webfeat.lib.ed.ac.uk/doi/abs/10.1080/14786435.2011.609152>
- [15] Cépas O and Canals B 2012 *Phys. Rev. B* **86**(2) 024434 URL <http://link.aps.org/doi/10.1103/PhysRevB.86.024434>

- [16] Kitaev A 2003 *Annals of Physics* **303** 2–30 ISSN 0003-4916 URL <http://www.sciencedirect.com/science/article/pii/S0003491602000180>
- [17] Wen X G 1991 *Phys. Rev. B* **44** 2664–2672
- [18] Ioffe L B, Feigel'man M V, Ioselevich A, Ivanov D, Troyer M and Blatter G 2002 *Nature* **415** 503–506
- [19] Zaanen J and Overbosch B J 2011 *Phil. Trans. Roy. Soc. A*: **369** 1599–1625 URL <http://rsta.royalsocietypublishing.org/content/369/1941/1599.abstract>
- [20] de Vries M A, McLaughlin A C and Bos J G 2010 *Physical Review Letters* **104** 177202 URL <http://link.aps.org/doi/10.1103/PhysRevLett.104.177202>
- [21] Tarzia M and Biroli G 2008 *EPL (Europhysics Letters)* **82** 67008 ISSN 0295-5075 URL <http://www.iop.org/EJ/abstract/0295-5075/82/6/67008>
- [22] Chen G, Pereira R and Balents L 2010 *Phys. Rev. B* **82** 174440 URL <http://link.aps.org/doi/10.1103/PhysRevB.82.174440>
- [23] Cussen E J, Lynham D R and Rogers J 2006 *Chemistry of Materials* **18** 2855–2866 URL <http://dx.doi.org/10.1021/cm0602388>
- [24] Aharen T, Greedan J E, Bridges C A, Aczel A A, Rodriguez J, MacDougall G, Luke G M, Imai T, Michaelis V K, Kroeker S, Zhou H, Wiebe C R and Cranswick L M D 2010 *Phys. Rev. B* **81** 224409 URL <http://link.aps.org/doi/10.1103/PhysRevB.81.224409>
- [25] Schiffer P and Daruka I 1997 *Phys. Rev. B* **56** 13712–13715 URL <http://link.aps.org/doi/10.1103/PhysRevB.56.13712>
- [26] Uemura Y J, Keren A, Kojima K, Le L P, Luke G M, Wu W D, Ajiro Y, Asano T, Kuriyama Y, Mekata M, Kikuchi H and Kakurai K 1994 *Phys. Rev. Lett.* **73** 3306–3309
- [27] Cannella V and Mydosh J A 1972 *Phys. Rev. B* **6** 4220–4237 URL <http://link.aps.org/doi/10.1103/PhysRevB.6.4220>
- [28] Wiebe C R, Greedan J E, Kyriakou P P, Luke G M, Gardner J S, Fukaya A, Gat-Malureanu I M, Russo P L, Savici A T and Uemura Y J 2003 *Phys. Rev. B* **68** 134410 URL <http://link.aps.org/abstract/PRB/v68/e134410>
- [29] Cherry M, Islam M S, Gale J D and Catlow C R A 1995 *J. Phys. Chem.* **99** 14614–14618 ISSN 0022-3654 URL <http://dx.doi.org/10.1021/j100040a007>
- [30] Baker P J, Lord J S and Prabhakaran D 2011 *J. Phys.: Cond. Matt.* **23** 306001 ISSN 0953-8984, 1361-648X URL <http://iopscience.iop.org/0953-8984/23/30/306001>
- [31] Singh R R P 2010 *Physical Review Letters* **104** 177203 URL <http://link.aps.org/doi/10.1103/PhysRevLett.104.177203>
- [32] Dodds S A, Gist G A, MacLaughlin D E, Heffner R H, Leon M, Schillaci M E, Nieuwenhuys G J and Mydosh J A 1983 *Phys. Rev. B* **28** 6209–6215 URL <http://link.aps.org/doi/10.1103/PhysRevB.28.6209>
- [33] Shpyrko O G, Isaacs E D, Logan J M, Feng Y, Aeppli G, Jaramillo R, Kim H C, Rosenbaum T F, Zsack P, Sprung M, Narayanan S and Sandy A R 2007 *Nature* **447** 68–71 ISSN 0028-0836 URL <http://dx.doi.org/10.1038/nature05776>